Proceedings of ICFDP7:
Seventh International Congress on Fluid Dynamics and Propulsion
December 18-20, 2001, Cairo, Egypt

ICFDP7-2001006

APPLICATION OF ENTROPY CONCEPT IN THE STUDY OF VELOCITY DISTRIBUTION FOR PIPE FLOW WITH DRAG REDUCING POLYMER ADDITIVES

M. F. Khalil, S.Z. Kassab, A.A. Elmiligui, and F.A. Naoum
Mechanical Engineering Department
Faculty of Engineering, Alexandria University, Alexandria, 21544
EGYPT

ABSTRACT
The equation of the velocity distribution based on probability and entropy concepts for Newtonian fluids is modified to obtain the velocity distribution through pipe under the condition of drag reduction. The proposed model needs only the knowledge of the friction loss coefficient (or the amount of drag reduction) to give the velocity distribution. The present study shows that, at certain solvent Reynolds number, the velocity distribution of the pipe flowing drag reducing fluids, equals to the velocity distribution of the solvent fluid, but at solvent Reynolds number that gives the same drag reducing friction loss coefficient.

1. INTRODUCTION
The velocity distribution is basic to all processes that take place in pipes and channels. Because of fluid viscosity, the various layers of flowing fluid, that is, the fluid at different radii in the pipe, travel at different velocities, as it is shown graphically in Fig.1.

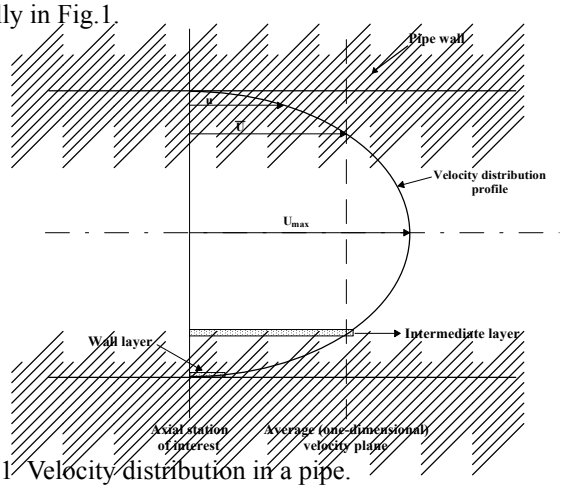

Fig. 1 Velocity distribution in a pipe.

In addition to Reynolds number; Re; that will serve as one indicator of the velocity distribution, there are, of course, other factors that also influence the velocity distribution. These factors are: the turbulence level in the flowing stream (flow is laminar or turbulent), the condition of the boundary wall surface (the wall is smooth or rough), and the proximity of the axial station in the pipe with respect to the pipe inlet (inlet effect). When the velocity profile no longer changes with distance from the inlet, the boundary layer is said to be fully developed. Namely, there are two flow regimes: laminar regime, and turbulent regime. Between these two regimes, there is necessarily a transition regime.

1.1 Velocity distribution in the laminar flow:
When the fluid can be considered to be flowing in layers or laminae, with the sole linkage between the layers taken to be based on momentum for set up as a result of molecular interactions, the flow is called laminar. This occurs when the pipe Reynolds number Re is below 2,000. In the fully developed stage, the velocity distribution can be considered by a parabola. However, the velocity distribution is given as the ratio of axial velocity, u, at such distance, r, from the pipe centerline to the maximum velocity (i.e., the velocity at the pipe centerline), U_{max}; as follows

$$\frac{u}{U_{max}} = 1 - \left(\frac{r}{R}\right)^2 \qquad 1$$

where, R (= D / 2) is the pipe radius; and D is the pipe diameter.

Fig. 2 shows the dimensionless laminar velocity profile for flow in a pipe. However, for laminar flow, since the protrusions are all contained within a laminar boundary layer, the pipe roughness does not influence the velocity distribution, and Eq.1 is still be right for rough pipes also.

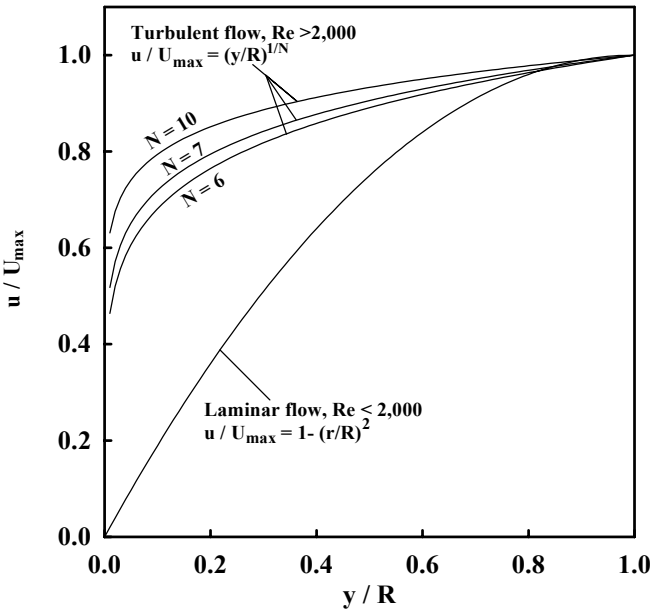

Fig. 2 Power law velocity profile for smooth pipe.

1.2 Velocity distribution in the transition flow:

Between laminar and turbulent regimes, there is necessarily a transition region. This has been found experimentally to be a function of pipe Reynolds number (Senecal and Rothfus 1953). Nominally, the value of Re that makes the inception of turbulence in pipes is about 2,000. For beyond this critical Reynolds number, the flow is bound to be turbulent. Much below the critical Reynolds number (~ 2,000), the flow will be laminar. The dramatic increase in the ratio of average (bulk) velocity, $\overline{U}$; to the maximum velocity, $U_{max,}$ above the critical Reynolds number is accompanied by a sudden increase in the pressure drop in the pipe (see Fig. 3).

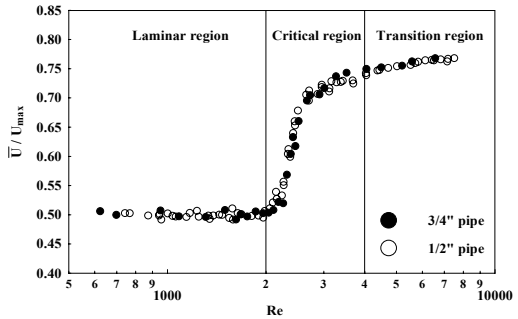

Fig. 3 The ratio U_{max} / $\overline{U}$ as a function of Re (Senecal and Rothfus 1953).

1.3 Velocity distribution in the turbulent flow:

When Reynolds number exceeds a critical value, nominally 2,000 for pipe flow, the flow deviates considerably from the laminar case. Momentum is now transferred radially, as well as, axially as a result of the mixing motion that accompanies the onset of turbulence (Benedict 1980).

Unlike the laminar flow case, we must be careful to distinguish between smooth and rough pipes in turbulent flow considerations, admitting that the method of delineating between these two boundary surface conditions is given only in part by the relative roughness ratio, e/D, where e is the absolute roughness. Once more, we are speaking of fully developed boundary layers, where the velocity distribution does not change with the axial position.

For the smooth pipe considerations, there are two laws for the velocity distribution: historically, the oldest of a smooth pipe velocity profile is the so-called "power law", and a slightly newer is the so-called "law of the wall" velocity. We will consider only the power law velocity profile.

Fig.2, again, presents the power law velocity in terms of u / U_{max} versus y / R, where y is the distance from the pipe wall, i.e., y = R - r. However, whereas only one curve is required to describe laminar flow, it is noted that a series of curves is needed to describe the turbulent flow, depending on pipe Reynolds number Re. The general form of these curves is

$$\frac{u}{U_{max}} = \left(\frac{y}{R}\right)^{1/N} = \left(1-\frac{r}{R}\right)^{1/N} \qquad 2$$

where, N is the reciprocal of the slope of the turbulent curves.

According to Eq. 2, two items of information are required to establish the turbulent velocity profile. These items are: the geometric factor (y / R), and the turbulent exponent (1 / N).

The quantity N is a function of Reynolds number Re, as seen from the fact that the data taken at different Re fall on different curves (see Fig.2). Although a functional relation between N and Re is not immediately apparent (Benedict 1980) an empirical relation between these two variables can be given, as in Table 1.

Table 1 Empirical relation between Re and N.

Re	4×10^3	1.1×10^5	1.1×10^6	3.2×10^6
N	6	7	8.8	10

Data from Benedict (1980)

However, the general power (1 / N) in Eq. 2 is usually replaced by the specific power (1 / 7), that is, N = 7. Hence, Eq. 2 is re-written as

$$\frac{u}{U_{max}} = \left(\frac{y}{R}\right)^{1/7} = \left(1-\frac{r}{R}\right)^{1/7} \qquad 3$$

and in this case, Eq. 3 is called the 1 / 7 th power law.

When the ratio u / U_{max} of Eq. 2 is integrated over the cross sectional area of the pipe, we obtain a dimensionless

volumetric average (bulk) velocity ratio, $\overline{U}$ / $U_{max,}$ in terms of exponent N as follows

$$Q = A\,\overline{U} = \int_0^R u\,(2\pi r)\,dr \qquad 4$$

where, Q is the volumetric flow rate; and A (= $\pi D^2/4$) is the pipe cross sectional area.

The general form of Eq. 4 is given as

$$\frac{\overline{U}}{U_{max}} = \frac{2N^2}{(N+1)(2N+1)} \qquad 5$$

It must be remembered that the power law given in Eq. 2 or 3 is for smooth pipe only. The velocity distributions for rough pipes are quietly differ than those for smooth pipes at the same Reynolds number. The difference depends upon the degrees of roughness. However, when the data of velocity distribution for both smooth and rough pipes are written in the form

$$\frac{U_{max} - u}{u^*} = f\left(\frac{y}{R}\right) \qquad 6$$

The velocity distribution curves versus the geometric factor (y / R) collapse to a single curve for all degrees of roughness, and for all values of Reynolds numbers. Here, u^* (= $\sqrt{\tau_w / \rho}$) is the friction velocity; τ_w is the wall shear stress; and ρ is the fluid density.

Prandtl showed that the form of Eq.6 is as follows

$$\frac{U_{max} - u}{u^*} = \frac{1}{K}\ln\left(\frac{y}{R}\right) \qquad 7$$

where, K is the von Karman's constant. Eq. 7 usually called as Prandtl's universal velocity distribution law.

However, Eq. 7 does not satisfy the boundary condition that u = 0 at the pipe wall, i.e., at r = R and y = 0, and hence, is incorrect near the pipe wall. Neither does it satisfy the boundary condition that du/dr = 0 at the pipe centerline, i.e., at r = 0 and y = 1. Therefor, the equation is also inaccurate near the pipe centerline. In addition, the velocity gradient given by Eq. 7 goes to infinity at the pipe wall, such a result would require that the shear stress become infinity large at the wall. Evidently, the universal law (Eq. 7) must cause to apply in a very thin region adjacent to the wall. Probably due to such complexity, Eq. 7 is still popular, and its deficiencies are often ignored in engineering applications, since it is considered adequate for providing the velocity over most of the flow region.

Empiricism has played a major role in the development of many power formulas with different exponents (or powers) for the streamwise time-mean velocity distribution in turbulent shear flows, whereas the logarithmic law velocity is well known for its theoretical soundness and universal validity. According to Barenblatt (1979), the logarithmic velocity distribution is based on the assumption of complete self-similarity of the flow in both the local and the global Reynolds number (i.e., Reynolds number based on the local flow variables and the cross section-averaged flow variables, respectively), whereas the power velocity distribution is formulated on the assumption of incomplete self-similarity in the local Reynolds number. Barenblatt further stated that for the logarithmic velocity distribution, dimensional analysis is sufficient for establishing self-similarity and determining the self-similar variables, whereas for the power velocity distribution, dimensional analysis is insufficient for establishing self-similarity and determining the self-similar variables. Insufficiency of the methodology in dimensional analysis to develop the power velocity distribution is thus reflected in the indeterminacy of the exponent and coefficient associated with the power law.

It is well known that the logarithmic velocity distribution can be approximated by the power velocity distribution in a large fraction of the boundary layer cross section (Hinze 1975), namely in the overlapping region of the inner law (i.e., the law of the wall) and the outer law (i.e., the velocity defect law). In other wards, one may theoretically generate various power flow formulas from the corresponding logarithmic velocity formula (Chen 1991). However, Chen developed a viable procedure to determine numerically the exponent and coefficient of the power law, using the logarithmic velocity distribution (or logarithmic flow formula) as a yardstick in the least squares approximation of the power velocity distribution (or power flow formula). The exponent and coefficient of the power law so determined were found to vary with the global Reynolds number and with the global relative roughness (i.e., based on the cross section-averaged) for hydraulically smooth flow and fully rough flows, respectively.

To overcome the boundary condition problems that arise when using Prandtl's universal law (Eq. 7), Chiu (1989, 1991), Chiu et al. (1993) and Chiu and Said (1995) applied the concept of entropy based on probability, developed previously by Chiu (1987, 1988), in modeling the vertical distributions of the flow velocity and shear stress in pipe and open channel flows. Chiu formulated the velocity distribution problem and related variables probabilitically and applied the variational principal to maximize the "entropy" as defined and used in the field of "information theory" (Shore and Johnson 1980). A velocity distribution equation derived by Chiu has advantages as an alternative to the existing Prandtl's universal law and power law velocity distribution equations for pipes, as well as open channels.

Araújo and Chaudhry (1998) investigated the applicability of the principle of maximum entropy obtained by Chiu (1987) in hydrodynamics, particularly in velocity distribution in open channels, by comparing the prediction of Chiu's entropy model with measured data. They found that the results of Chiu's entropy model are in good agreement with the measured data. Moreover, Chiu's

entropy model performs better than the other existing model (logarithmic model) in practically all flow regions. They concluded that the better velocity predictions obtained without prior adjustment on the basis of observed data attest to the validity of the principle of maximum entropy in hydraulics and encourage its further use.

The concept of entropy based on probability applied by Chiu (1988) and Chiu et al. (1993), will use in the present study for flows of solutions of drag reducing polymer additives, as well as drag reducing non-polymeric additives (surfactants, and solid suspensions) in pipes. However, there are two types of non-polymeric additives that produce a considerable reduction in the pressure drop accompanying turbulent flow in pipes. These drag reducing fluids are the solutions of surface-active-agents (surfactants) or soap solutions, and the dilute suspensions of properly sized solid particles. Patterson et al. (1969) presented a good article about the drag reduction phenomenon caused by each of these three types of additives (polymers, surfactants, and suspensions).

2. REVIEW OF DRAG REDUCING VELOCITY DISTRIBUTION IN PIPES:

Many investigators have studied the velocity distribution across pipes (Eissenberg and Bogue 1964, Virk et al. 1967, Patterson and Florez 1969, Rudd 1972, McComb and Rabie 1982, Kato and Mizunuma 1983, McComb and Chan 1985, Tam et al. 1992, Bewersdorff and Thiel 1993, Myska et al. 1996, and den Toonder et al. 1997), flowing solutions of drag reducing additives (polymers, surfactants, and suspensions). Their results are in general agreement. However, all studies of velocity distribution under the condition of drag reduction showed that the main action of the drag reducing additive is to increase the thickness of the viscous sublayer in the boundary layer, or to create an elastic sublayer (for polymers and surfactants) between the viscous sublayer and the turbulent core, as it was shown by Virk (1971). Hence, the law of wall velocity profile gives a clear picture about the effects of drag reducing additives. The effect of drag reducing fluids on the law of the wall velocity profile is discussed, in detail, in Naom (2000).

Although there are many studies about the effects of drag reducing additives on the law of the wall velocity distribution, but only few studies (Eissenberg and Bogue 1964, Goren and Norbury 1967, Virk et al. 1967, Patterson and Florez 1969, Nicodemo et al. 1969, Rudd 1972, and Myska et al. 1996) were existed about the effect of drag reducing additives on the power law velocity distribution.

Bogue and Metzner (1963) found that Newtonian and non-visco-elastic non-Newtonian fluids (although these include drag reducing fluids with higher concentrations) had essentially the same velocity profiles in turbulent flow. However, Hoyt (1972) reported that friction reducing polymer additives produce a complicated velocity profile.

Eissenberg and Bogue (1964) obtained semi-empirical relationships for friction coefficients and velocity profiles for a dilute (does not produce any drag reduction) and a concentrated (drag reducing) aqueous thoria suspension. They found that the velocity profile of a dilute suspension of thoria, is similar to the Newtonian (solvent) profile at the same Re. While for the concentrated thoria suspension, the relationship shown that the decrease of the friction coefficient cause a change in the velocity distribution profile.

Zandi and Rust (1965) and Murthy and Zandi (1969) proposed a method for the prediction of turbulent velocity profile across the pipe cross section for purely viscous (Newtonian and non-Newtonian) fluids, as well as fluids exhibit drag reducing behavior as polymers, surfactants, and suspensions. Their method is semi-analytical, and is verified with previously reported experimental data. However, they treated the drag reducing solutions as non-Newtonian fluids due to the high concentrations of these solutions (flow index less than unity). Despite that velocity equations by Zandi and Rust (1965) and Murthy and Zandi (1969) satisfied the boundary conditions at the pipe wall (velocity is vanished) and at the center of the pipe (slope is zero), but, during the comparison, these equations gave prediction values less than the observed data in the vicinity of the pipe wall.

Goren and Norbury (1967) depending on their measurements of velocity profiles for dilute solutions of polyethylene oxide polymer, made the following observations:

1. In the case of high drag reduction amount (~ 72%), the relation between u / U_{max} and y / R indicates that the velocity gradient for the polymer solution in close proximity to the wall is smaller than that for solvent water. At values of y / R approximately between 0.08 and 0.3, this trend reverses. Beyond that, the velocity profile becomes very flat and yields a value of centerline velocity U_{max} smaller than that for the solvent water, for a given average (bulk) velocity $\overline{U}$.
2. The velocity defect results showed a close agreement between polymer solutions and solvent water in the region between the three-quarter pipe radius ($y/R = 0.2$) and the centerline ($y / R = 1$). Toward the wall, however, there is a distinct effect. The negative slope ($[U_{max} - u] / u^*$) : y/R) increases in magnitude with increasing in the polymer concentration. This effect begins at $y / R \leq 0.25$.

   However, the flatter velocity profile, was again found by many investigators (Virk et al. 1967, Patterson and Florez 1969, Nicodemo et al. 1969, Sayer and Metzner 1969, Rudd 1972, and Myska et al. 1996) based on measurements in solutions of several kinds of polymers and surfactants, flowing under different conditions.

   Nicodemo et al. (1969) concluded that the flatness of velocity profile is due to the increase in efficiency of

turbulent momentum transfer comparing with Newtonian solvent fluids. Seyer and Metzner (1969) experimentally found that the velocity flatness is dependent on the increased isotropy of the turbulent field of the drag reducing fluid. They reported that these effects appear to be a result of increases in the time scale of the radial fluctuations caused by the fluid properties.

Rudd (1969) measured the polymeric velocity profile using laser Doppler anemometer (LDA) technique. Rudd (1972) reported that the reason for the flatter drag reducing velocity profile is that, since the wall stress is lower for the drag reducing fluids, the velocity defect is less at a similar position in the flow. Rudd concluded that the polymer additive does not have any affect upon the turbulence in the core region of pipe flow. The change in the velocity profile is solely due to the change in the wall stresses. This suggested that the effect of the additive is confined to the region of pipe flow close to the wall. The results of Rudd are similar to those obtained previously by Virk et al. (1967).

Another significant discrepancy between the velocities of solvents and drag reducing additives, is that the centerline to average velocity ratio $U_{max} / \overline{U}$ for drag reducing fluid is slightly lower than that for Newtonian solvent fluid. This result was found experimentally by many investigators (Patterson and Florez 1969, Nicodemo et al. 1969, Kenney and Thwaites 1971, and Rudd 1972).

Kenney and Thwaites (1971) reported that the velocity profile for a drag reducing polymer solution at a given average velocity may be obtained by assuming that it can be derived by modifying the velocity profile for Newtonian solvent fluids, flowing at the lower average velocity which gives the same wall shear stress as the dilute polymer solution.

Virk (1975) reviewed many results of velocity profiles obtained by many investigators as Goren and Norbury (1967), Rollin and Seyer (1972), as well as his previous results (Virk et al. 1967). For the results presented in a velocity defect plot, that is, $(U_{max} - u) / u^*$ against y / R, he showed that polymer solutions with lower velocity defect profiles identically the same as Newtonian fluids for $1.0 > y / R > 0.05$. As the amount of drag reduction is increased, the velocity defect remains Newtonian toward the axis ($1.0 > y / R > 0.2$), but is greater than Newtonian toward the wall ($y / R < 0.2$). At maximum drag reduction, the velocity defect exceeds Newtonian over the entire pipe cross section.

Recently Myska et al. (1996) present velocity profiles for several kinds of solutions of drag reducing surfactants (Habon-G; Ethoquad T/13; and Arquad 18/50), as well as solvent water, measured by LDA technique. The measurements were made at a range of concentrations and velocities (not reported) at which the maximum drag reduction for the Habon-G and Arquad 18/50 solutions was reached, which is not the case for Ethoquad T/13 solution. The main feature of the velocity for all surfactant solutions in the region of turbulent core, is that, beside its flatness, the dimensionless velocity $u / \overline{U}$ is greater than that for solvent water. However, this result contradicts all other experimental results obtained previously which showed that $u / \overline{U}$ for additives solutions is smaller than that for solvents. They concluded that the presence of surfactants suppress the eddy formation and propagation near the pipe wall. However, they experimentally found that tangential and radial turbulence intensities for drag reducing surfactants are much lower than those for solvent water, while axial (longitudinal) intensities are lower (at $y / R > 0.15$), but surprisingly, not at the wall. In the wall region (at $y / R < 0.15$), axial turbulence intensities for all surfactant solutions were higher than those for solvent water.

Although there are many models describe the drag reducing velocity in terms of the law of the wall equation (Eissenberg and Bouge 1964, Virk et al. 1970, and Tam et al. 1992) but from the review of previous results, one can write that, there is no equation predicting the velocity distribution profile for the drag reducing fluids in terms of power law velocity, in which all available models (Bogue and Metzner 1963, Zandi and Rust 1964, and Murthy and Zandi 1969) treated the drag reducing fluids as non-Newtonian fluids. However, the drag reducing fluids with lower concentrations (i.e., several PPMW), have properties nearly similar to Newtonian (solvent) fluids, and do not behave as non-Newtonian fluids.

3. ANALYTICAL EQUATION FOR DRAG REDUCING VELOCITY DISTRIBUTION IN PIPES:

In a pipe flow, the time-averaged velocity varies in the vertical y-direction. Let u ($0 \le u \le U_{max}$) be the time-averaged and, therefore, time-invariant velocity on an isovel (equi-velocity surfaces), which is assigned a value ξ ($\xi_0 \le \xi \le \xi_{max}$). The term u is zero along an isovel that has ξ value equal to ξ_0, which represents the solid pipe wall. In addition, u is U_{max}, the maximum value of u, at ξ equal to ξ_{max}, which occur at the pipe centerline. The velocity u increases monotonically with the spatial coordinate ξ ranged from ξ_0 to ξ_{max}.

In the probabilistic formulation, both ξ and u are consider as random variables with probability functions as q and p, respectively. Suppose all values of the spatial variable ξ between ξ_0 and ξ_{max} are equally likely, so that the probability function of ξ is uniform on the interval [ξ_0, ξ_{max}], that is,

$$q(\xi) = 1 / (\xi_{max} - \xi_0)$$

and zero outside this interval. Then, the probability of the velocity being less than or equal to u, or the (cumulative)

distribution function P of u, can be derived according to DeGroot (1970) as

$$P(u) = \int_0^u p(u)\,du = \int_0^u p[G(\xi)]\,du = \int_{\xi_0}^{G^{-1}(u)} q(\xi)\,d\xi = \frac{\xi - \xi_0}{\xi_{max} - \xi_0} \qquad 9$$

This means that, if ξ is randomly sampled between ξ_0 and ξ_{max}, and the corresponding u [= G (ξ)] is obtained, then the probability of velocity between u and u + du is p(u) du.

According to Eq. 9 and the definition of probability density function p(u), then

$$p(u) = \frac{dP(u)}{du} = \frac{dP(u)}{d\xi}\,\frac{d\xi}{du} = \frac{1}{\xi_{max} - \xi_0}\,\frac{d\xi}{du} \qquad 10$$

Eqs. 9 and 10 indicate that, once equations of p (u) and ξ are determined, a velocity distribution equation can be derived to describe the structure of variation of u with ξ and, hence, y coordinate.

One approach to determining the probability density function p (u) is the entropy-maximizing principle, which is already a well-established method used in statistics, statistical mechanics, and information theory (Jaynes 1957). The method in the present case is to select p (u) that maximizes the entropy

$$H(u) = -\int_0^{U_{max}} p(u)\,\ln p(u)\,du \qquad 11$$

subject to the constraints

$$\int_0^{U_{max}} p(u)\,du = 1 \qquad 12$$

and

$$\int_0^{U_{max}} u\,p(u)\,du = \overline{U} \qquad 13$$

Eq.13 is equivalent to satisfying the condition that u must be distributed over the cross-sectional area so that $\overline{U}$ A = Q. The method is based on the postulate that a system under a steady equilibrium condition tends to maximize the entropy. In information theory, the entropy as defined by Eq. 11 is interpreted as the average information content per message (sample data) about u and is used as a measure of uncertainty, or how close an a priori probability distribution is to the uniform. The entropy maximization is equivalent to making the probability distribution as uniform as possible while satisfying the prevailing constraints. Additional interpretations of entropy can be found in the relevant literature by Chiu (1987).

The method of the calculus of variations that may be determined p (u) in the preceding equations is to solve

$$\frac{\partial}{\partial p}[-p\,\ln p + \lambda_1\,p + \lambda_2\,(u\,p)] = 0 \qquad 14$$

in which λ_1 and λ_2 are Lagrange multipliers. Eq.3A-14 gives

$$p(u) = e^{\lambda_1 - 1}\,e^{\lambda_2\,u} \qquad 15$$

Substitution of Eq. 15 into 12 and 13 yields

$$e^{\lambda_1 - 1} = \lambda_2\,(e^{\lambda_2\,U_{max}} - 1)^{-1} \qquad 16$$

and

$$\overline{U} = U_{max}\,e^{\lambda_2 U_{max}}\,(e^{\lambda_2 U_{max}} - 1)^{-1} - \frac{1}{\lambda_2} \qquad 17$$

Solution of a differential equation obtained from Eqs. 10 and 15, using the boundary condition that u = 0 at $\xi = \xi_0$ gives

$$u = \frac{1}{\lambda_2}\ln\left(1 + \frac{\lambda_2}{e^{\lambda_1 - 1}}\,\frac{\xi - \xi_0}{\xi_{max} - \xi_0}\right) \qquad 18$$

As shown in Eqs. 16 and 17, if U_{max} and $\overline{U}$ are known (measured), the two parameters λ_1 and λ_2 can be determined, but if not, the two parameters can be determined by the method of least squares using velocity distribution data.

The term $e^{\lambda_1 - 1}$, according to Eq. 15, is the value of the probability density function p (u) at u = 0, and is related to λ_2 and U_{max} by Eq. 16. Therefore, Eq. 18 can be expressed in the form

$$\frac{u}{U_{max}} = \frac{1}{M}\,\ln\left[1 + (e^M - 1)\,\frac{\xi - \xi_0}{\xi_{max} - \xi_0}\right] \qquad 19$$

in which M [= $\lambda_2\,U_{max}$] is a dimensionless entropy parameter that, according to Eqs. 10 and 15, is

$$M = \ln\frac{p(U_{max})}{p(0)} = \ln\frac{\left(\frac{du}{d\xi}\right)_{\xi = \xi_0}}{\left(\frac{du}{d\xi}\right)_{\xi = \xi_{max}}} \qquad 20$$

Hence, M is a measure of the uniformity of the probability and velocity distributions. Eq. 19 was derived by Chiu's for velocity distribution in pipes and channels (Chiu 1988, and Chiu et al. 1993). It has two parameters, λ_2 and U_{max}.

For a pipe flow of axial symmetry, in which isovels are concentric circles (Chiu et al. 1993), ξ should be

$$\xi = (\pi R^2 - \pi r^2) / (\pi R^2) = 1 - (r / R)^2 \qquad 21$$

which is the ratio of the area in which the velocity is less than or equal to u (ξ) to the total area of the pipe cross section. With ξ defined by Eq. 21, thus, $\xi_0 = 0$ and $\xi_{max} = 1$, and Eq. 19 becomes

$$\frac{u}{U_{max}} = \frac{1}{M}\,\ln[1 + (e^M - 1)\,\xi] \qquad 22$$

Eq. 22 satisfies the two important boundary conditions, that is, u = 0 at r = R (i.e., $\xi = \xi_0 = 0$) and du / dr = 0 at r = 0 (i.e., $\xi = \xi_{max} = 1$), which the Prandtl's universal law (Eq. 7) fails to do. Again, unlike Eq. 7, Chiu's velocity distribution

(Eq. 19) does not give the velocity gradient that goes to infinity at the pipe wall.

The probability concept, as represented by Eq. 9, clearly shows that the velocity u in a pipe of axial symmetry varies with 1 - (r / R)^2, not with 1 - (r / R), which is the distance from the wall as indicated by Prandtl's universal law (Eq. 7). The entropy of the distribution p (u / U_{max}), obtained by Eq. 11 with u replaced by u / U_{max} and the upper limit of integration replaced by unity, is a function of only the entropy parameter M. Smaller values of M correspond to more uniform patterns of probability distribution p (u / U_{max}), and greater values of entropy parameter M correspond to less uniform velocity distribution, as shown graphically in Fig. 4.

By equating the sum of pressure and gravity forces with the frictional resistance, the wall shear stress can be written as

$$\tau_{ws} = \rho\left(u^*\right)^2 = \rho g D h_{f_s} / (4L) \qquad 23$$

in which, g is the gravitational acceleration, h_f is the head loss due to friction, L is the pipe length over which friction factor loss is $h_{f,}$ and subscript s denotes solvent fluids.

Eq. 23 is for Newtonian (solvent) fluids that do not exhibit drag reducing behavior. Now we will introduce the effect of drag reducing additives in Eq. 23. As mentioned above, the effect of additive solution is to reduce the frictional losses by a certain amount called the drag reduction amount DR.

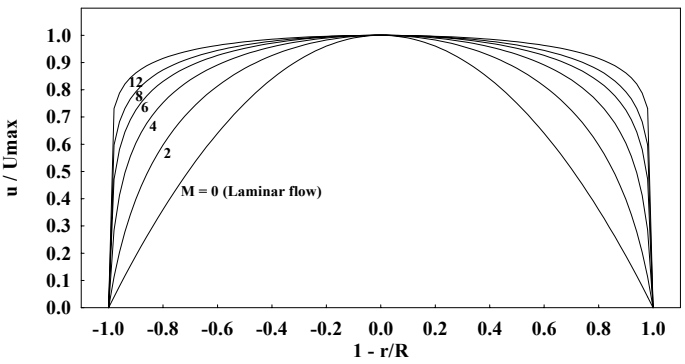

Fig.4 Velocity distribution as a function of entropy parameter M (Chiu et al. 1993)**.**

Percentage drag reduction in pipe flow, DR%, is customarily quantified by comparing friction coefficient values obtained with and without drag reducing additive, i.e., f_s and f_d, respectively, at the same solvent Reynolds number (i.e., depending on the physical properties of solvent). More exactly

$$DR\% = [(f_s - f_d) / f_s] \times 100 \Big|_{\text{at the same solvent Re}} \qquad 24$$

The percentage amount of drag reduction (Eq. 24), is rewritten in terms of head loss as

$$DR\% = \left[\left(\tau_{w_s} - \tau_{w_d}\right)/\tau_{w_s}\right] \times 100 = \left[\left(h_{f_s} - h_{f_d}\right)/h_{f_s}\right] \times 100 \Big|_{at the same \mathrm{Re}} \qquad 25$$

Hence, Eq. 23 becomes

$$\tau_{w_d} = \tau_{w_s}(1 - DR) = \rho g D h_{f_s}(1 - DR)/(4L) = \rho g D h_{f_d}/(4L) \qquad 26$$

where, subscript d denotes drag reducing fluids. Eq. 26 is for drag reducing fluids. However, for the special case when the drag reducing fluid does not exhibit any drag reducing behavior (sometimes at lower Reynolds number), i.e., the amount of drag reduction DR = 0, the obtained correlation, Eq. 26, yields that for Newtonian (solvent) fluids, i.e., Eq. 23.

Based on the balance between the shear stress and diffusion of momentum at the pipe wall

$$\tau_w = \rho \varepsilon_0 \left(\frac{-du}{dr}\right)_{r=R} \qquad 27$$

where, ε_0 is the momentum transfer coefficient at the pipe wall, which is equal to the kinematic viscosity ν of the fluid if the flow is laminar, or if the flow is turbulent with a viscous sublayer (i.e., the pipe is hydraulically smooth). For a turbulent flow in rough pipes, ε_0 is greater than ν, and varies with the pipe roughness and fluid turbulence. With the velocity distribution represented by Eq. 22, and ξ by Eq. 21, the velocity gradient can be written as

$$\frac{du}{dr} = -\frac{U_{max}}{M} \frac{(e^M - 1)}{1 + (e^M - 1)\left[1 - (r/R)^2\right]} \qquad 28$$

which is zero at r = 0, as it should be, at the wall, Eq. 28 becomes

$$\left(\frac{du}{dr}\right)_{r=R} = -\frac{2 U_{max}\left(e^M - 1\right)}{M R} \qquad 29$$

which, unlike the velocity gradient given by Prandtl's universal law (Eq. 7) remains finite. According to L'Hopital's rule, as M approaches zero, Eqs. 28 and 29 become (-2 U_{max} r / R^2) and (-2 U_{max} / R), respectively. Eqs. 23 (or 26), 27, and 29 give the head loss due to friction over the pipe length L, for both Newtonian and drag reducing fluids, as

$$h_f = 32\left(\frac{e^M - 1}{M}\right)\left(\frac{U_{max}}{\overline{U}}\right)\left(\frac{\nu}{D\overline{U}}\right)\left(\frac{\varepsilon_0}{\nu}\right)\left(\frac{L}{D}\right)\left(\frac{\overline{U}^2}{2g}\right) \qquad 30$$

By comparing Eq. 30 with the Darcy-Weisbach relation, and using Eq. 22 for $\overline{U}$ / U_{max}, the friction factor can be obtained as

$$f = 32\left(\frac{e^M - 1}{M}\right)\left(\frac{U_{max}}{\overline{U}}\right)\left(\frac{\nu}{D\overline{U}}\right)\left(\frac{\varepsilon_0}{\nu}\right) = 32\,\frac{F(M)}{Re}\left(\frac{\varepsilon_0}{\nu}\right) \qquad 31$$

in which

$$F(M) = \left(e^M - 1\right)\left[M\,e^M\left(e^M - 1\right)^{-1} - 1\right]^{-1} \qquad 32$$

Fig. 5 shows that F(M) increases with entropy M. Eq. 31 gives the friction factor of three dimensionless parameters, M, Re, and ε_0/ν. The entropy parameter M represents the velocity distribution pattern and, hence, the rates of energy and momentum transport. In smooth pipes, a viscous sublayer exists at the wall and, hence, $\varepsilon_0 = \nu$. If the flow is laminar, hence, $\varepsilon_0 = \nu$ and f = 64/Re, and Eq. 31 yields F (M) = 2, or from Eq. 32, and according to L'Hopital's rule, M = 0 (see Fig. 5).

Despite that Eq. 31 is general relation, i.e., is used for Newtonian (solvent) fluids as well as for drag reducing fluids, but, it must be noted that the use of friction coefficient for drag reducing fluids will not give the correct velocity distribution for this fluids. In other words, any trivial correction due to lower friction factors in drag reducing fluids, as a direct effect of these fluids, is not sufficient to correlate the data of drag reducing velocity profile. Hence, replacing f_s with f_d, is a trivial solution to obtain the correct value of entropy M that determines the drag reducing velocity distribution.

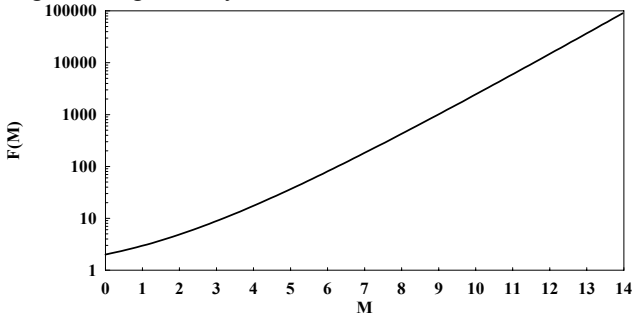

Fig. 5 Function F(M) (Chiu et al. 1993).

In the present study we developed a new Reynolds number and called it "equivalent Reynolds number". The equivalent Reynolds number; $Re_{eq,}$ is equal to the Newtonian Reynolds number that -according to the Prandtl's equation- gives the value of drag reducing friction coefficient. In mathematical form, this means that Re_{eq} is obtained from

$$\sqrt{1/f_d} = 2\,\log\left(Re_{eq}\sqrt{f_d}\right) - 0.8 \qquad 33$$

For the special case when the amount of drag reduction DR = 0, Eq. 33, again, yields friction coefficient for Newtonian (solvent) fluids. Now, Eq. 31, for flow of both solvent and drag reducing fluids in smooth pipe, becomes

$$f = 32\,\frac{F(M)}{Re_{eq}} \qquad 34$$

The equivalent Reynolds numbers Re_{eq}, for flowing of drag reducing fluid at several amounts of drag reduction DR, are shown graphically in Fig. 6.

As M approaches zero, according to L'Hopital's rule, Eq. 22 becomes

$$\frac{u}{U_{max}} = \xi = 1 - \left(\frac{r}{R}\right)^2 \qquad 35$$

which is identical to the parabolic velocity distribution for the laminar flow of Newtonian fluid presented by Eq. 1. As mentioned above (see Fig. 4), no difference from the Newtonian (solvent) behavior is observed for drag reducing fluids in the laminar flow, that is, the drag reducing friction coefficient follows that for Newtonian fluids (Virk et al. 1967, Virk 1971, and den Toonder et al. 1997). Therefore, no change in the velocity profile will be occur for the laminar flow of drag reducing fluids comparing with Newtonian fluids, and in this case, Eq. 35 can again be used for drag reducing fluids without any correction.

If Eq. 9 is used to represent P (u), the average value of u, that is the volumetric mean velocity $\overline{U}$, can be obtained as the mathematical expectation of u (Chiu 1988), and expressed the ratio $\overline{U}$ to U_{max} as a function of M

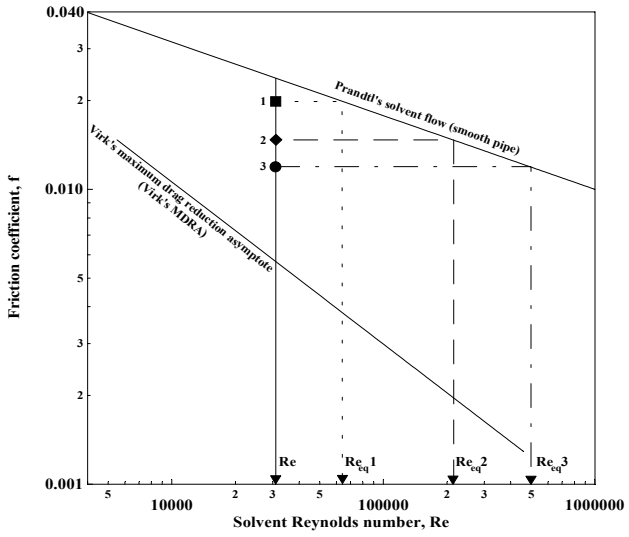

Fig. 6 Equivalent Reynolds numbers Re_{eq} for flowing of drag reducing fluids at several amounts of drag reduction DR.

$$\frac{\overline{U}}{U_{max}} = e^{M}\,(e^{M}-1)^{-1} - \frac{1}{M} \qquad 36$$

As M approaches zero (that is, the flow is laminar), according to L'Hopital's rule, Eq. 36 gives $U_{max} = 2\,\overline{U}$ which is, again, identical to the parabolic velocity distribution for the laminar flow of Newtonian fluids.

Combining Eqs. 19 and 22, the velocity distribution in terms of $u / \overline{U}$ at distance r from the pipe centerline can be expressed as

$$\frac{u}{\overline{U}} = \frac{\ln\left[1+ (e^{M}-1)\,\xi\right]}{M\,e^{M}\,(e^{M}-1)^{-1} - 1} \qquad 37$$

The expected values of u^2 and u^3, give the momentum and energy coefficients, also can be obtained as functions of entropy M (Chiu 1991). This shows that the transport of mass, momentum, and energy can be interpreted in terms of entropy parameter M.

In Eq. 36, the ratio $U_{max} / \overline{U}$ is decreased by the increase in value of entropy M, as it is shown in Fig. 7. Note that in this figure, when the entropy parameter M = 0 (i.e., the flow is laminar), the ratio $U_{max} / \overline{U} = 2$. At certain Reynolds number, since the friction coefficient for drag reducing fluids is less than that for solvents alone, hence, according to Eqs. 32 to 34, the entropy M is greater for drag reducing fluids, and hence, smaller $U_{max} / \overline{U}$ ratio for drag reducing fluids comparing with solvents. This agrees well with the data of velocity profiles for drag reducing fluids obtained by many investigators (Patterson and Florez 1969, Nicodemo et al. 1969, Kenney and Thwaites 1971, and Rudd 1972).

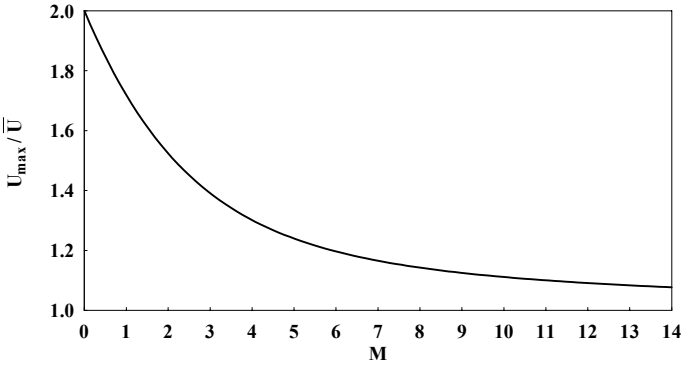

Fig. 7 The maximum to average velocity ratio $\mathbf{U_{max} / \overline{U}}$, as a function of entropy M.

Fig. 8 shows the velocity distribution $u / \overline{U}$ (Eq. 37) for both drag reducing fluids with several amounts of drag reduction DR = 20; 40; 60; and 80%, and solvent fluid (i.e., DR = 0%), at constant Reynolds number (Re = 30,000). Eqs. 32 to 34 are used to compute the three dimensionless parameters $Re_{eq,}$ F (M); and M. The entropy parameter M is greatly increased from 4.32 at DR = 0% (solvent fluid) to about 14.15 for drag reducing fluid at maximum drag reduction (DR = 80%). This is due to the large increase in value of Re_{eq}. However, due to the increase in value of M, the ratio $U_{max} / \overline{U}$ is decreased from 1.28 at DR = 0% to about 1.08 at DR = 80%. Two features are observed in Fig. 8 for the increase of drag reduction amount, and hence, the increase of entropy M: the velocity distribution profile is much flatter in the turbulent core region, and again is much steeper in the vicinity of the wall.

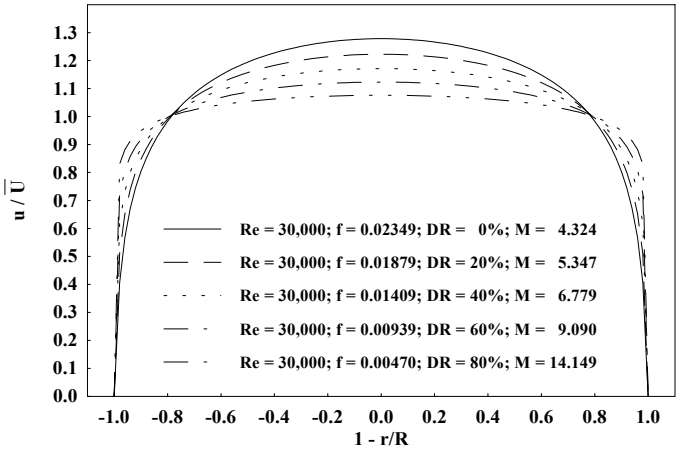

Fig. 8 Drag reducing velocity distribution for several drag reduction amounts.

4. COMPARISON OF THE EXPERIMENTAL VELOCITY DATA WITH THE PRESENT CORRELATION

To test the validity of the proposed equation, Eqs.22 or 37, in prediction the velocity distribution profile for both drag reducing fluids as well as Newtonian (solvent) fluids. Comparisons are made for several independent sets of experimental data obtained by previous investigators for velocity profiles of solutions of drag reducing additives as polymers (Virk et al. 1967, Patterson and Florez 1969, Seyer and Metzner 1969, Nicodemo et al. 1969, and Rudd 1972), surfactant (Patterson and Florez 1969), and suspensions (Eissenberg and Bogue 1964), flowing in pipes under different Reynolds numbers, different concentrations, and different pipe diameters. Table 2 presents the data used. Figs. 9 to 14 show the comparisons.

The following observations could be drawn from the comparisons shown in Figs. 9 to 14:

1. The proposed equation, in general, is in good agreement with the experimental data of velocity profiles for drag reducing fluids, as well as Newtonian (solvent) fluids. One indication of the degree of agreement between the calculated results and the measured results for each velocity distribution, is the percentage error in the ratio of maximum to average velocity $U_{max} / \overline{U}$, which is given as

$$\text{Error}\,\% = \left(1 - \frac{\left.\frac{U_{max}}{\overline{U}}\right|_{Exp}}{\left.\frac{U_{max}}{\overline{U}}\right|_{Cal}}\right) \times 100 \qquad 38$$

The percentage error computed from Eq. 38 is reported in Table 2. For 26 independent sets of experimental data used in comparison, the percentage error is ranged from -5.53 to +6.09%. However, the slight deviation between the calculated and measured results is due to many factors. These include, uncertainty of the measurements, variations on the measuring techniques (as Pitot tubes, hot film anemometer, bubble streak photography, and LDA), as well as limitation of the present model. Many investigators (Smith et al. 1967, Friehe and Schwarz 1969, and Mushimaru and Tomita 1974) observed the experimental errors in data measured by classical instruments as Pitot tubes, and hot film anemometer. The experimental studies reported that Pitot tubes behave anomalously in the turbulent flow of dilute polymer solutions. The discrepancy in the Pitot tube readings increases with the absolute velocity; the molecular weight and concentration of polymer; and with decreasing Pitot tube diameter. Hot film measurements indicate that the heat transfer is poorer in polymer solutions than in solvent alone and exhibits abrupt transitions over which the heat transfer coefficient may vary by threefold. However, the previous investigators showed some deviation of the calculated average (bulk) velocity $\overline{U}_{Integ}$ (or flow rate) by integrating each measured velocity profile, from the average (bulk) velocity $\overline{U}_{Weigh}$ (or flow rate) measured by time weighing, for both drag reducing and solvent fluids. Table 3 presents the magnitude of the velocity deviation for the measuring data used in comparison.

Table 3 The deviation of velocity profile data.

Investigator (s)	**Deviation (%)** $\text{Dev}\,\% = \left(1 - \frac{\overline{U}_{Integ}}{\overline{U}_{Weigh}}\right) \times 10$
Virk et al. (1967)	– 0.6 to + 4.6
Patterson and Florez (1969)	– 3.1 to + 2.1
Seyer and Metzner (1969)	– 6.3 to + 5.9
Nicodemo et al. (1969)	– 1.8 to + 3.8

2. The proposed (Modified Chiu's) equation predicts well the flatness of velocity distribution profile for drag reducing fluids, comparing with solvents, in the region of turbulent core. Figs. 11, 12, and 14 present, respectively, the flat velocity profile in turbulent core region, under the drag reducing conditions such that for 100 PPMW of polymer PAM (ET-597) at Re = 144,000 obtained by Seyer and Metzner (1969), for 100 PPMW of polymer PAM (Separan AP-30) at Re = 50,000 obtained by Rudd (1972), and for 10,000 PPMW of soap (aluminum dioleate) at Re = 53,000 obtained by Patterson and Florez (1969), comparing with solvent profiles at nearly the same Reynolds numbers. The flatness of velocity profile increases by the increase in the value of entropy parameter M, that is, by the increase in the amount of drag reduction DR or solvent Reynolds number Re. Outside the turbulent core, it can be noted that, at the same Reynolds number, the velocity profiles for drag reducing fluids are much steeper than those for solvent fluids, in the vicinity of the wall. This is an indication of boundary layer thickening, due to the turbulence suppression near the pipe wall, as the main action of drag reducing agents. Figs. 9 to 14 show that the proposed (modified Chiu's) equation predicts well the steeping of the drag reducing velocity profiles in the vicinity of the pipe wall. Again, The steeping of velocity profile increases by the increase in the value of entropy parameter M.
3. In Fig. 13, Nicodemo et al. (1969) used the equation of Bogue and Metzner (1963) to correlate their drag reducing results. The model of Bogue and Metzner, which can be cast in the following form

$$\frac{u}{\overline{U}} = \sqrt{f/8}\left(5.57\log(y/R) + 3.63\right) + 0.05\exp\left\{\frac{-\left[(y/R) - 0.8\right]^2}{0.15}\right\} + 0.984 \qquad 39$$

is plotted in Fig. 13 by the dashed line, and again is used for comparison with the proposed equation. It is obvious from this figure that, while Bogue and Metzner's equation, Eq. 39, correlates well the experimental data for the solvent water results, but for polymer results, there is a deviation between two results. Bogue and Metzner developed their model, to be valid for both Newtonian and non-Newtonian purely viscous fluids (i.e., non-drag reducing fluids). However, Nicodemo et al. (1969) used Bogue and Metzner's equation to correlate their drag reducing results since the friction factor appears explicitly, so that, any trivial correction due to lower friction factors in drag reducing fluids is taken into account directly, but Fig. 13 shows truly that the correction of friction factor as a direct effect of polymer additives is not sufficient to correlate the data of polymeric velocity profile. Hence, in the present study, the assumption of equivalent Reynolds number Re_{eq}, which causes an increase in the value of entropy M (see Eqs. 32 to 34) as a unique parameter of Chiu's equation, seems to be valid for predicting the velocity profile of drag reducing fluids.
2. Regarding Virk's data (Fig. 10), it can be noted that in turbulent flow, when the polymeric fluid follows the

friction relation of Newtonian fluid, that is, the polymeric fluid does not produce any drag reduction (DR = 0), hence, there is no change in the velocity profile comparing with that for Newtonian fluids. This mathematically means that the entropy M is obtained for $Re = Re_{eq}$. However, this case is similar to the laminar flow condition, in which the drag reducing fluids behave as Newtonian ones, and hence, no change in velocity profile comparing with Newtonian (solvent) fluids. In this case, the Chiu's equation for laminar flow velocity, Eq. 35, can again be used for drag reducing fluids without any correction.

5. CONCLUSION

The velocity distribution equation based on probability and entropy concepts is modified in the present study to allow the pipe velocity distribution under the condition of drag reduction to be obtained.

The present study shows that, at certain solvent Reynolds number Re, the velocity distribution of the pipe flowing drag reducing fluids, equals to the velocity distribution of the Newtonian (solvent) fluids, but at solvent Reynolds number The present model needs, only, the knowledge of the friction loss coefficient (or the amount of drag reduction) to give the velocity distribution profile.

The results show that:

1. Turbulent velocity profile for polymer solution can be predicted by only one equation.
2. The proposed model predicts well the flatness of velocity profile for drag reducing fluids in the core region, and its steeping in the vicinity of the pipe wall.
3. It verifies the experimental observation that the ratio of maximum velocity to average (bulk) velocity $U_{max} / \overline{U}$ for drag reducing fluids is smaller than that for solvent fluids, at the same Reynolds number. For 26 independent sets of experimental data obtained by previous investigators and used in comparison, the deviation of calculated $U_{max} / \overline{U}$ ratios, from the measured ones, is ±6%.

REFERENCES

Araújo, J.C., and Chaudhry, F.H., 1998, "Experimental evaluation of 2-D entropy model for open-channel flow", *J. Hyd. Eng.*, *ASCE*, Vol. 124, No. 10, PP. 1064-1067.

Barenblatt, G.I., 1979, *Similarity, self-similarity, and intermediate asymptotics*, Consultants Bureau, New York, N.Y., USA.

Benedict, R.P., 1980, *Fundamentals of pipe flow*, A Wiley-Interscience Publication, John Wiley & sons; Inc., New York, N.Y., USA.

Bewersdorff, H.W., and Thiel, H., 1993, "Turbulence structure of dilute polymer and surfactant solutions in artificially roughened pipes", *Appl. Sci. Res.*, Vol. 50, Nos. 3-4, PP. 347-368.

Bogue, D.C., and Metzner, A.B., 1963, "Velocity profiles in turbulent pipe flow, Newtonian and non-Newtonian fluids", *I & EC Fund.*, Vol. 2, No. 2, PP. 143-149.

Chen, C.L., 1991, "Unified theory on power laws for flow resistance", *J. Hyd. Eng.*, *ASCE*, Vol. 117, No. 3, PP. 371-389.

Chiu, C.L., 1987, "Entropy and probability concepts in hydraulics", *J. Hyd. Eng.*, *ASCE*, Vol. 113, No. 5, PP. 583-599.

Chiu, C.L., 1988, "Entropy and 2-D velocity distribution in open channels", *J. Hyd. Eng.*, *ASCE*, Vol. 114, No. 7, PP. 738-756.

Chiu, C.L., 1989, "Velocity distribution in open channel flow", *J. Hyd. Eng.*, *ASCE*, Vol. 115, No. 5, PP. 576-594.

Chiu, C.L., 1991, "Application of entropy concept in open channel flow study", *J. Hyd. Eng.*, *ASCE*, Vol. 117, No. 5, PP. 615-627.

Chiu, C.L., and Said, C.A.A., 1995, "Maximum and mean velocities and entropy in open-channel flow", *J. Hyd. Eng.*, *ASCE*, Vol. 121, No. 1, PP. 26-35.

Chiu, C.L., Lin, G.F., and Lu, J.M., 1993, "Application of probability and entropy concepts in pipe-flow study", *J. Hyd. Eng.*, *ASCE*, Vol. 119, No. 6, PP. 742-756.

DeGroot, M.H., 1975, *Probability and statistics*, Addison-Wesley Publishing Co., Reading, Mass.

den Toonder, J.M.J., Hulsen, M.A., Kuiken, G.D.C., and Nieuwstadt, F.T.M., 1997, "Drag reduction by polymer additives in a turbulent pipe flow: numerical and laboratory experiments", *J. Fluid Mech.*, Vol. 337, PP. 193-231.

Eissenberg, D.M., and Bogue, D.C., 1964, "Velocity profiles of thoria suspensions in turbulent pipe flow", *AIChE J.*, Vol. 10, No. 5, PP. 723-727.

Friehe, C.A., and Schwarz, W.H., 1969, "The use of Pitot-static tubes and hot-film anemometers in dilute polymer solutions", *Proc. Symp. on Viscous Drag Reduction (1968)*, C.S. Wells (ed.), PLENUM PRESS, New York, N.Y., PP. 281-296.

Goren, Y., and Norbury, J.F., 1967, "Turbulent flow of dilute aqueous polymer solutions", *J. Basic Eng.*, *Trans. ASME*, Vol. 89, No. 4, PP. 814-822.

Hinze, J.O., 1975, *Turbulence*, McGraw-Hill Book Co., New York, N.Y., USA.

Hoyt, J.W., 1972, "The effect of additives on fluid friction", *J. Basic Eng.*, *Trans. ASME*, Vol. 94, No. 2, PP. 258-285.

Jaynes, E.T., 1957, "Information theory and statistical mechanics I.", *Physics Rev.*, Vol. 106, No. 4, PP. 620-630.

Kato, H., and Mizunuma, H., 1983, "Frictional resistance in fiber suspensions (1st report, pipe flow)", *Bull. JSME*, Vol. 26, No. 212, PP. 231-238.

Kenney, C.N., and Thwaites, G.R., 1971, "Axial dispersion in a drag reducing fluid in turbulent flow", *Chem. Eng. Sci.*, Vol. 26, No. 4, PP. 503-508.

McComb, W.D., and Chan, K.T.J., 1985, “Laser-Doppler anemometer measurements of turbulent structure in drag-reducing fiber suspensions”, *J. Fluid Mech.*, Vol. 152, PP. 455-478.

McComb, W.D., and Rabie, L.H., 1982, “Local drag reduction due to injection of polymer solutions into turbulent flow in a pipe - Part II: Laser-Doppler measurements of turbulent structure”, *AIChE J.*, Vol. 28, No. 4, PP. 558-565.

Murthy, V.R.K., and Zandi, I., 1969, “Turbulent flow of non-Newtonian suspensions in pipes”, *J. Eng. Mech. Div.*, *Proc. ASCE*, Vol. 95, No. EM1, PP. 271-288.

Mushimaru, Y., and Tomita, Y., 1974, “A study on the flows of dilute polymer solutions (4th report, on the velocity measurements by a Pitot tube method)”, *Bull. JSME*, Vol. 17, No. 114, PP. 1594-1601.

Myska, J., Zakin, J., and Chara, Z., 1996, “Viscoelasticity of a surfactant and its drag-reducing ability”, *Appl. Sci. Res.*, Vol. 55, No. 4, PP. 297-310.

Naoum, F.A., 2000,”Effect of polymer additives on sprinkler irrigation system performance”, Ph. D. thesis, Faculty of Engineering, Alexandria University, Egypt.

Nicodemo, L., Acierno, D., and Astarita, G., 1969, “Velocity profiles in turbulent pipe flow of drag-reducing liquids”, *Chem. Eng. Sci.*, Vol. 24, No. 8, PP. 1241-1246.

Patterson, G.K., and Florez, G.L., 1969, “Velocity profiles during drag reduction”, *Proc. Symp. on Viscous Drag Reduction (1968)*, C.S. Wells (ed.), PLENUM PRESS, New York, N.Y., PP. 233-250.

Patterson, G.K., Zakin, J.L., and Rodrigues, J.M., 1969, “Drag reduction - Polymer solutions, soap solutions and solid particle suspensions in pipe flow”, *I & EC*, Vol. 61, No. 1, PP. 22-30.

Rollin, A., and Seyer, F.A., 1972, “Velocity measurements in turbulent flow of viscoelastic solutions”, *Can. J. Chem. Eng.*, Vol. 50, PP. 714-718.

Rudd, M.J., 1969, “Measurements made on a drag reducing solution with a laser velocimeter”, *Nature*, Vol. 224, Nov. 8, PP. 587-588.

Rudd, M.J., 1972, “Velocity measurements made with a laser dopplermeter on the turbulent pipe flow of a dilute polymer solution”, *J. Fluid Mech.*, Vol. 51, Pt. 4, PP. 673-685.

Senecal, V.E., and Rothfus, R.R., 1953, “Transition flow of fluids in smooth tubes”, *Chem. Eng. Prog.*, Vol. 49, No. 10, PP. 533-538.

Seyer, F.A., and Metzner, A.B., 1969, “Turbulence phenomena in drag reducing systems”, AICHE J., Vol. 15, No.3, pp. 426-434.

Shore, J.E., and Johnson, R.W., 1980, “Axiomatic derivation of the principle of maximum entropy and the principle of maximum cross-entropy”, *Trans. Inform. Theory, IEEE,* Vol. II-26, No. 1, PP. 623-656.

Smith, K.A., Merrill, E.W., Mickley, H.S., and Virk, P.S., 1967, “Anomalous Pitot tube and hot film measurements in dilute polymer solutions”, *Chem. Eng. Sci.*, Vol. 22, PP. 619-626.

Tam, K.C., Tiu, C., and Keller, R.J., 1992, “A general correlation for turbulent velocity profiles of dilute polymer solutions”, *J. Hyd. Res.*, Vol. 30, No. 1, PP. 117-142.

Virk, P.S., 1971, “An elastic sublayer model for drag reduction by dilute solutions of linear macromolecules”, *J. Fluid Mech.*, Vol. 45, Pt. 3, PP. 417-440.

Virk, P.S., 1975, “Drag reduction fundamentals - Journal review”, *AIChE J.*, Vol. 21, No. 4, PP. 625-656.

Virk, P.S., Merrill, E.W., Mickley, H.S., Smith, K.A., and Mollo-Christensen, E.L., 1967, “The Toms phenomenon: turbulent pipe flow of dilute polymer solutions”, *J. Fluid Mech.*, Vol. 30, Pt. 2, PP. 305-328.

Virk, P.S., Mickley, H.S., and Smith, K.A., 1970, “The ultimate asymptote and mean flow structure in Toms phenomenon”, *J. Appl. Mech.*, *Trans. ASME*, Vol. 92, No. 2, PP. 488-493.

Zandi, I., and Rust, R.H., 1965, “Turbulent non-Newtonian velocity profiles in pipes”, *J. Hyd. Div.*, *Proc. ASCE*, Vol. 91, No. HY6, PP. 37-55.

Table 2 Summary of turbulent velocity profile measurements on drag reducing solutions used in the present study.

Investigator (s)	Year	D (mm)	C (PPMW)	Re	f	$\overline{U}$ m/s	$U_{max}/\overline{U}$ Exp.	$U_{max}/\overline{U}$ Cal.	Error (%)	DR (%)	Re_{eq}	M	Measurement technique	Fluid
Eissenberg et al. [#]	1963	40.6	0	177,829	.01628	3.58	1.199	1.191	+0.65	0	177,829	6.149	Pitot	Solvent water
		40.6	0	162,630	.01832	3.27	1.186	1.190	- 0.37	0	162,630	6.184	Pitot	Solvent water
		40.6	973	31,473	.02028	2.98	1.175	1.240	- 5.53	12.7	57,215	4.990	Pitot	Thoria-oxide suspension
		40.6	1,830	8,873	.02476	2.60	1.266	1.294	- 2.21	22.4	24,027	4.090	Pitot	Thoria-oxide suspension
Virk et al.	1967	32.1	0	50,000	.02089	1.42	1.234	1.247	- 1.08	0	50,000	4.852	Pitot	Solvent water
		32.1	1,000	36,000	.02251	1.40	1.251	1.267	- 1.22	0	36,000	4.514	Pitot	PEO (Polyox N-3000)
		32.1	0	250,000	.01498	7.06	1.172	1.183	- 0.92	0	250,000	6.396	Pitot	Solvent water
		32.1	1,000	180,000	.01044	7.06	1.158	1.134	+2.06	34.6	1,923,493	8.451	Pitot	PEO (Polyox N-3000)
Patterson & Florez	1969	25.4	0	41,000	.02185	1.83	1.218	1.259	- 3.34	0	41,000	4.648	Pitot	Solvent cyclohexane
		25.4	0	83,000	.01871	3.76	1.215	1.222	- 0.62	0	83,000	5.362	Pitot	Solvent cyclohexane
		25.4	2,000	27,000	.02263	1.83	1.329	1.268	+4.60	6.0	35,160	4.489	HFA	PIB (Vistanex L-200)
		25.4	2,000	55,000	.01473	3.78	1.207	1.178	+2.36	28.0	272,730	6.549	HFA	PIB (Vistanex L-200)
		25.4	4,000	27,000	.01830	3.75	1.296	1.217	+6.09	24.0	92,230	5.473	HFA	PIB (Vistanex L-200)
			10,00			3.81	1.149	1.216	+5.50	42	856,031	7.667	HFA	Soap (Aluminum-dioleate)

		25.4	0	53,000	.01196					.0				
Seyer &	1969	25.4	0	160,000	.01582	5.64	1.200	1.197	+0.24	0	160,000	5.982	Bubble	Solvent water
Metzner		25.4	100	13,500	.02740	0.57	1.251	1.316	- 5.14	6.7	17,780	3.808	streak	PAM (ET-597)
		25.4	100	144,000	.00893	6.10	1.155	1.119	+3.13	45.0	5,183,443	9.406	photography	PAM (ET-597)
Nicodemo et al.	1969	30.4	0	--	.02014	2.93	1.210	1.238	- 2.34	0	59,090	5.023	Pitot	Solvent water
		30.4	500	--	.01392	1.81	1.145	1.170	- 2.15	- -	368,251	6.844	Pitot	PAM (ET-597)
		30.4	1000	--	.01435	1.83	1.135	1.174	- 3.45	- -	313,195	6.685	Pitot	PAM (ET-597)
		20.0	0	--	.02148	2.47	1.225	1.254	- 2.39	0	44,175	4.725	Pitot	Solvent water
		20.0	500	--	.01389	2.52	1.200	1.169	+2.56	- -	372,655	6.856	Pitot	PAM (ET-597)
		20.0	1000	--	.01382	2.55	1.185	1.168	+1.38	- -	382,240	6.881	Pitot	PAM (ET-597)
		20.0	1500	--	.01722	2.50	1.210	1.205	+0.39	- -	123,532	5.765	Pitot	PAM (ET-597)
Rudd	1972	12.7 s	0	50,000	.02700	3.53 I	1.163	1.230	- 5.13	0	50,000	5.187	LDA	Solvent water
		12.7 s	100	50,000	.01386	3.75 I	1.126	1.164	- 3.40	48.7	437,948	7.047	LDA	PAM (Separan AP-30)

PEO = polyethylene oxide polymer; PAM = polyacrylamide polymer; PIB = polyisobutylene polymer (dissolved in cyclohexane).
Soap (Aluminum-dioleate) = non-aqueous surfactant solution, dissolved in toluene.
HFA = hot film anemometer, LDA = laser Doppler anemometer.
[#] = data from Eissenberg and Bogue (1963), and Zandi and Rust (1965).
(I) = obtained by integration; (s) = square pipe; (--) = no data found; *Error (%) = computed from Eq. 38.

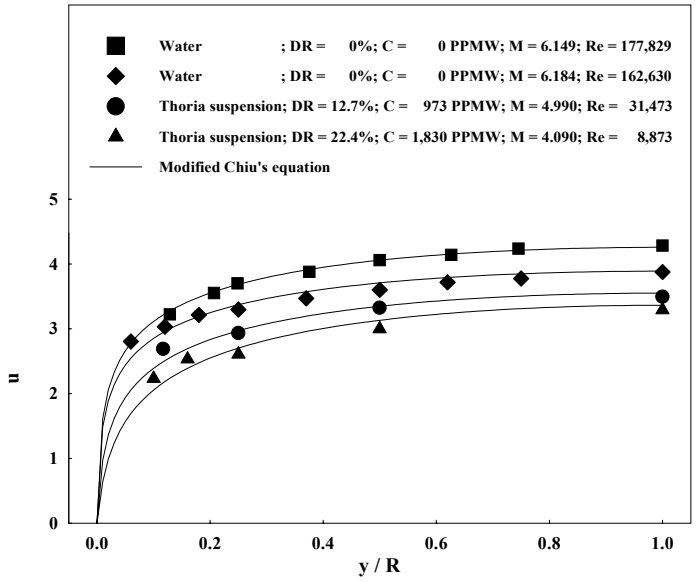

Fig. 9 Comparison with experimental data of Eissenberg and Bogue (1964), and Zandi and Rust (1965).

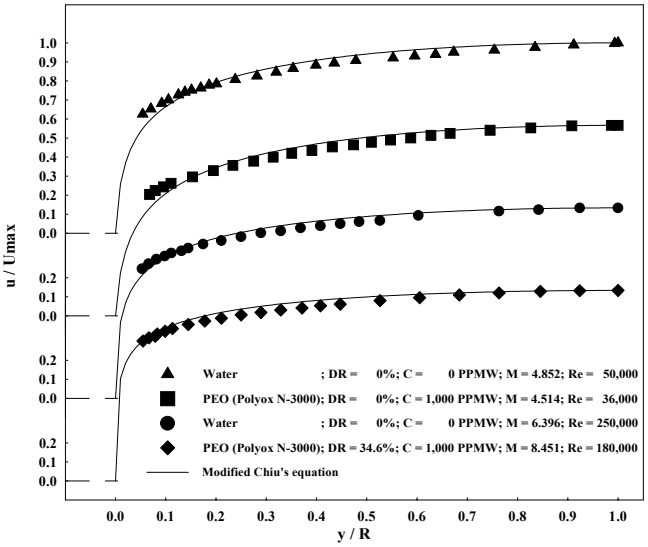

Fig. 10 Comparison with experimental data of Virk et al. (1967).

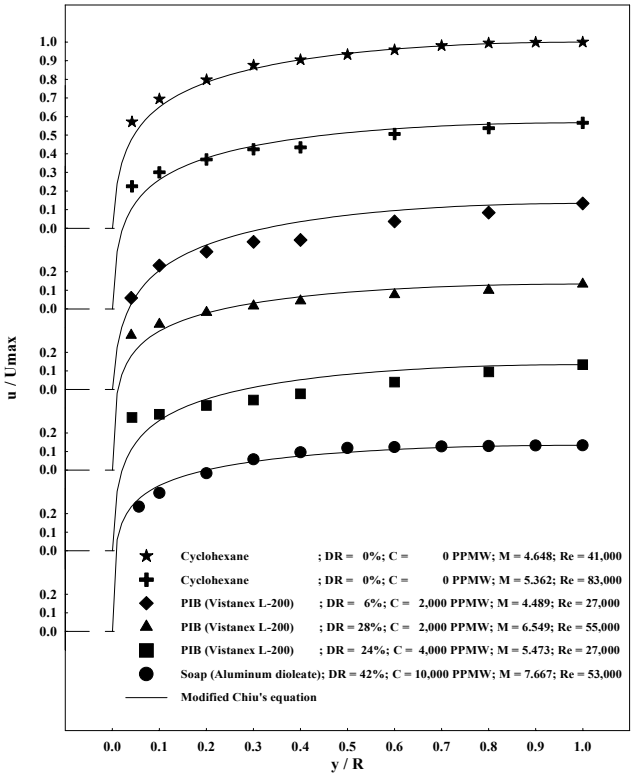

Fig. 11 Comparison with experimental data of Patterson and Florez (1969).

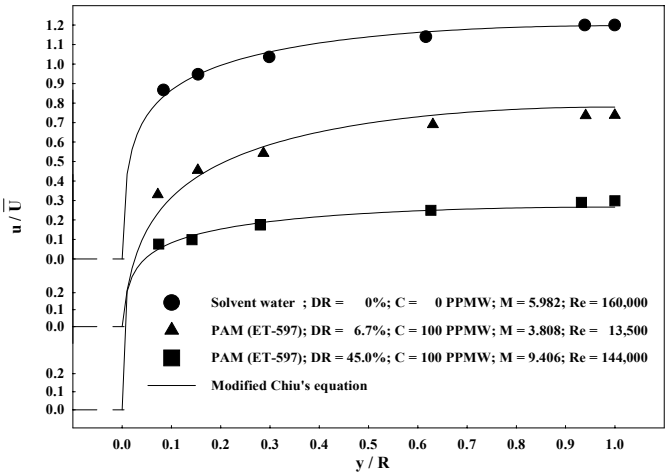

Fig. 12 Comparison with experimental data of Seyer and Metzner (1969).

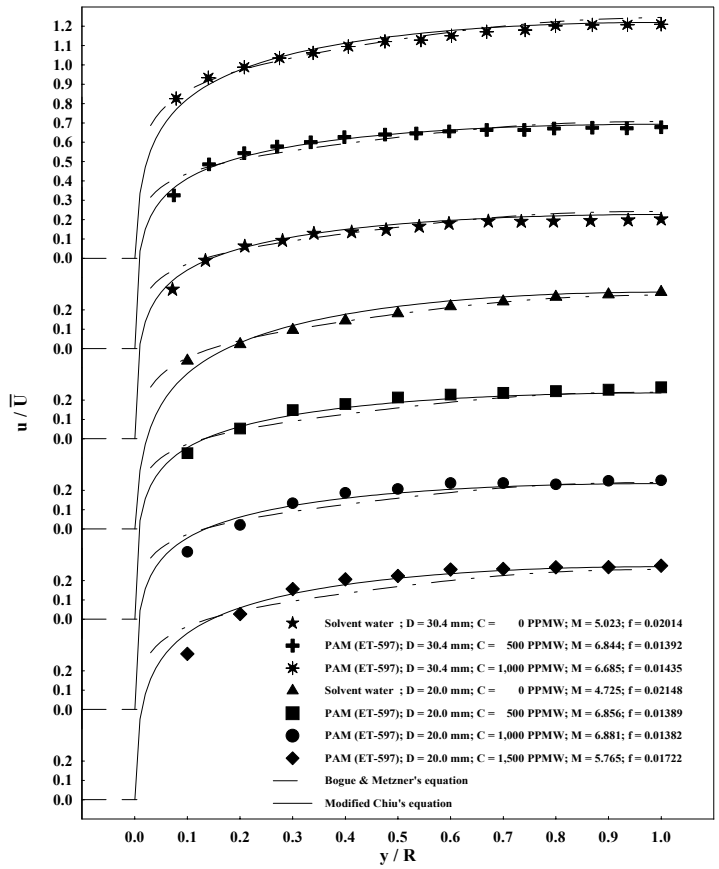

Fig. 13 Comparison with experimental data of Nicodemo et al. (1969).

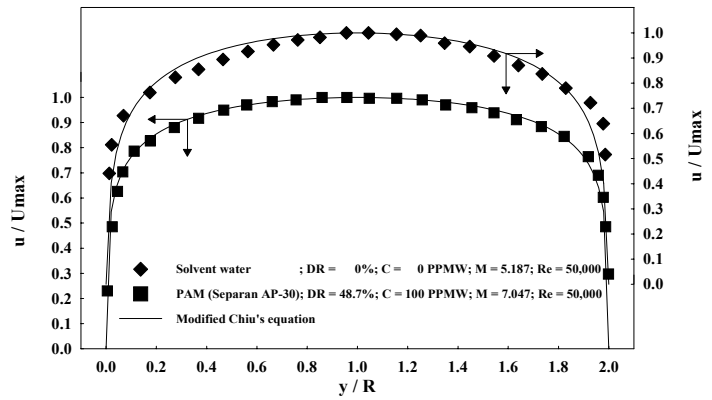

Fig. 14 Comparison with experimental data of Rudd (1972).